GAS Journal of Engineering and Technology (GASJET)

Volume 3 | Issue 1, 2026 Homepage: https://gaspublishers.com/gasjet-home/ ISSN: 3048-5800

Predictive Modelling of Residual Axial Capacity in Rockfall-Damaged Hollow RC Piers: A State-of-the-Art Review

MD Nishat Hasan[*1], MD Masud Rana[2], MD Saymun Hossain Shawon[3] & Sajid Ahmed[4]

ORCID: 0009-0002-5580-1027;[1] 0009-0006-0728-9099;[2] 0009-0002-4327-5306;[3] 0009-0009-7701-8464;[4]

[1&3]School of Civil Engineering, Southwest Jiaotong University, Chengdu 610031, China
[2]School of Civil and Transportation Engineering, Hohai University, Nanjing 210098, China
[4]School of Transportation and Civil Engineering, Nantong University, Jiangsu 226019, China

Received: *10.01.2026* | ***Accepted:*** *28.01.2026* | ***Published:*** *30.01.2026*

***Corresponding Author:** MD Nishat Hasan

DOI: *10.5281/zenodo.18431254*

Abstract **Review Article**

Hollow reinforced concrete piers in mountainous bridges face severe rockfall hazards causing localized panel damage and global instability, yet current design codes lack rockfall assessment protocols. This review synthesizes recent research on residual vertical load-carrying capacity prediction following rockfall impact. A critical finding is the dual failure mechanism: small rockfalls (diameter less than 1.8 meters) induce front-panel slab-action rupture with width approximately 947 mm, while large rockfalls (diameter 1.8 meters or greater) activate side-panel shear with width approximately 1388 mm. Advanced machine learning surrogates achieve exceptional accuracy (coefficient of determination 0.996) with computational speedup of one million times compared to traditional finite element analysis. Earthquake-rockfall cascade hazards reduce residual capacity by 83 percent in a non-additive manner, reflecting synergistic damage interaction. Parametric studies identify residual normalized deflection at the impact location as the optimal engineering demand parameter with correlation coefficient 0.92 to residual capacity. Performance-based design frameworks incorporating Monte Carlo vulnerability assessment enable practical rockfall-resistant pier design. Critical gaps remain in machine learning generalization to new geometries, standardization of damage indices, and integration of geological hazard characterization with structural analysis.

Keywords: rockfall impact, hollow RC piers, residual axial capacity, machine learning surrogates, performance-based design, vulnerability assessment.

Introduction

Hollow reinforced concrete piers in mountainous regions offer material efficiency but face severe rockfall hazards causing catastrophic failures (Z. Liu et al., 2024),(Zhao et al., 2023),(Wu et al., 2025). Current design codes provide no rockfall protocols, creating significant regulatory gaps that leave engineers without standardized assessment methodologies. The residual vertical load-carrying capacity metric, defined as $RVLCC = N_r / N_0 \times 100\%$, quantifies post-impact pier strength where N_r is the axial capacity after impact and N_0 is the undamaged initial capacity (G. Zhang et al., 2025),(Fan et al., 2019). Serviceability

thresholds establish that piers retaining high RVLCC can sustain essential services, piers with moderate reduction require repair before traffic restoration, and low RVLCC signals critical failure risk necessitating complete closure. Hollow piers exhibit temporally and mechanically distinct response stages during rockfall impact (Zhao et al., 2024),(Z. Liu et al., 2025). The local phase occurring from 0 to 5 milliseconds features extreme stresses and strain rates ranging from 10^1 to $10^2\,s^{-1}$ activate concrete strain-rate hardening (Liu Zhanhui et al., 2020),(Dhote et al., 2025). Simultaneously, stress waves propagate radially outward from the impact zone. The global phase occurring from 5 to 100 milliseconds involves overall pier stiffness mobilization, causing lateral displacement and side-panel damage. The rupture width of the front panel ω_r serves as the most reliable single predictor of residual capacity in rockfall-impacted hollow piers (Zhao et al., 2023),(Zhong et al., 2023). A critical finding from recent parametric studies is that rockfall diameter fundamentally alters the local failure mechanism with profound implications for design rules (Zhao et al., 2024). Small rockfalls with diameter less than 1.8 meters induce slab-action failure in the front panel with rupture width approximately 947 mm, while large rockfalls with diameter greater than or equal to 1.8 meters activate side-panel shear failure with rupture width approximately 1388 mm (Mo et al., 2025),(Jibson et al., n.d.). This distinction arises because small-diameter rockfalls concentrate contact pressure on the front panel exclusively, whereas large-diameter rockfalls contact both front and side panels, activating the full cross-sectional lateral stiffness and fundamentally altering the damage distribution pattern.

Earthquake damage presets piers for impact failure through distributed cracking and reduced confinement (Ma et al., n.d.),(J. Zhang, Mo, et al., 2025),(Technical Background Report, 2002). For maximum credible earthquake ground motion followed by rockfall at velocity 20 m/s and height 8.5 m, the RVLCC under earthquake alone reaches approximately 4.2×10^4 KN but drops dramatically to 0.7×10^4 KN under the cascade scenario. This 83 percent synergistic reduction reflects non-additive damage mechanisms where earthquake-induced cracking and reduced confinement diminish the pier's ability to withstand subsequent shear and impact stresses in ways that cannot be simply superposed (J. Zhang, Mo, et al., 2025). While the immediate mechanics of impact are complex, the long-term perspective reveals further vulnerabilities. In many mountainous regions, which are also often coastal or subject to de-icing salts, RC piers face the dual threats of rockfall and chloride-induced steel corrosion (Wu et al., 2025). The degradation of material properties over time specifically the corrosion of stirrups can exacerbate the damage caused by a rockfall event occurring decades into the structure's service life. Recent studies suggest that after 60 years of service, the residual bearing capacity post-impact can decrease by over 47% compared to a newly constructed pier, primarily due to the loss of confinement integrity (Wu et al., 2025).

This review paper aims to bridge the gap between isolated mechanical studies and practical predictive modelling. By synthesizing findings on impact dynamics, cascading hazards, and long-term deterioration, it evaluates the efficacy of current empirical and computational tools. The ultimate objective is to provide a unified framework for predicting RVLCC, thereby enabling engineers to make rapid, data-driven decisions regarding bridge safety and post-disaster operability.

Computational Methodologies: LS-DYNA and Machine Learning

The LS-DYNA nonlinear explicit finite element analysis code has become the de facto standard for rockfall-impact analysis because it excels at capturing transient impact phenomena with strong material nonlinearity, geometric nonlinearity, and sophisticated contact algorithms (Z. Liu et al., 2024),(Liu Zhanhui et al., 2020). Pier geometry is discretized using eight-node solid hexahedra elements with maximum element size of 25 mm established through convergence testing. Longitudinal reinforcement and stirrups employ Hughes-Liu beam elements with perfect bond between concrete and rebars enforced through the constrained Lagrange contact method. Material constitutive models include strain-rate-sensitive

plasticity for concrete using MAT_CONCRETE_DAMAGE_REL3 that captures strain-hardening at high strain rates relevant to rockfall impact where strain rates range from 10 to $1000 s^{-1}$ (Liu Zhanhui et al., 2020). Dynamic increase factors of 1.25 to 1.75 for compressive strength and 2.0 to 3.5 for tensile strength are typical for these strain-rate ranges. Reinforcement is modelled using isotropic strain-hardening plasticity with yield strength appropriate to the steel grade, with strain-rate enhancement per Cowper-Symonds law. Contact uses the automatic surface-to-surface algorithm activated when rockfall surface approaches pier surface within one element size distance.

Table 1 LS-DYNA Computational Framework

Parameter	**Specification**
Element Type	8-node hexahedra, 25 mm maximum size
Concrete Model	MAT_CONCRETE_DAMAGE_REL3
Steel Model	Isotropic strain-hardening
DIF (Compression)	1.25–1.75
DIF (Tension)	2.0–3.5
Contact	AUTOMATIC_SURFACE_TO_SURFACE

The "Dynain restart method" provides an essential specialized computational approach for predicting cascade-hazard scenarios where earthquake-induced damage precedes rockfall impact (Zhao et al., 2024),(Ma et al., n.d.). This technique involves two sequential finite element runs. The first step performs quasi-static earthquake analysis where the pier undergoes nonlinear lateral cyclic loading simulating target ground motions, capturing progressive concrete cracking, rebar yielding, and cumulative damage. At conclusion of earthquake loading, the deformed geometry, damaged material properties with reduced elastic modulus and degraded strength, and internal stress state are saved in a restart file. The second step initializes a new LS-DYNA run that inherits the earthquake-damaged state as initial condition, with subsequent rockfall impact analysis proceeding on this pre-damaged structure. This approach elegantly captures interaction between earthquake and rockfall damage without requiring excessive computation to simultaneously model both processes. The critical finding from cascade-hazard studies shows that cascade events reduce RVLCC by 83 percent in a non-additive manner, meaning the combined damage far exceeds the arithmetic sum of individual damage extents, reflecting synergistic interaction between damage mechanisms (J. Zhang, Mo, et al., 2025),(Chen et al., 2020). The relationship between rupture width and residual capacity can be expressed in Equation (1) (Zhao et al., 2023),(Zhong et al., 2023):

$$N_r = N_0\left[1-\left(\frac{\omega_r}{a-2c_1}\right)^{0.85}\left(\frac{\omega_r}{2a+2b-2c_1-2c_2}\right)^{0.50}\right] \quad R^2 = 0.90 \tag{1}$$

Where N_r is the residual axial capacity, N_0 is the initial capacity, ω_r is the rupture width, a and b denote the section width and height, and c_1, c_2 are the panel thicknesses. Eq (1) relates the rupture width w_r to

the residual capacity reduction, achieving excellent agreement with finite element results.

A transformative development in 2024–2025 literature is the systematic deployment of machine learning surrogates to predict peak rockfall impact force, circumventing expensive finite element simulations for parameter variation studies (J. Zhang, Jing, et al., 2025),(LIU Zongfeng et al., 2020),(J. Zhang, Mo, et al., 2025). The hybrid convolutional neural network combined with support vector machine architecture comprises several interconnected components. The input layer incorporates four rockfall parameters including mass, impact velocity, diameter, and impact height, which are normalized to the range zero to one and fed into the network. Convolutional layers perform feature extraction via convolution kernels typically comprising three to five kernels per layer with kernel size three by three or five by five. These layers learn hierarchical features capturing nonlinear interactions between input parameters. Pooling layers using max pooling or average pooling reduce dimensionality and computational cost while preserving essential features. Fully connected layers then connect the pooled features to a hidden representation space. The output stage replaces traditional fully connected output layers with support vector regression, which optimizes the margin around predicted values and enhances generalization.

A representative dataset comprises 134 training samples and 33 test samples, often augmented through data-generation techniques (J. Zhang, Mo, et al., 2025). The Adam optimizer with learning rate 0.001 and decay factor 0.01 trains for 250 iterations. Resulting metrics typically achieve root mean square error approximately 442 kilonewtons with R^2 approximately 0.96 on the training set and R^2 approximately 0.96 on the test set. The neural network output relationship is expressed in Equation (2), which combines convolutional feature extraction with support vector regression:

$$F_{impact} = \sigma\left(\sum_{i=1}^{n} w_i h_i + b\right) \quad (2)$$

where F_{impact} is the predicted peak impact force, w_i are the weight matrices from support vector regression layer, h_i are the hidden features from convolutional layers, b is the bias term, and σ is the activation function. Eq (2) combines convolutional feature extraction with support vector regression to predict peak impact forces. The speedup compared to LS-DYNA reaches one million times(J. Zhang, Jing, et al., 2025),(LIU Zongfeng et al., 2020).

Beyond impact-force prediction, the emerging frontier encompasses machine-learning surrogates for the complete residual bearing-capacity prediction pipeline. Box-Behnken design provides 46 parameter combinations that are augmented via Tabular Generative Adversarial Network to 167 samples(J. Zhang, Jing, et al., 2025). The resulting XGBoost machine learning model on test data achieves exceptional performance metrics documented in Table 2:

Table 2 XGBoost Surrogate Performance

Metric	Value
R2	0.996
RMSE	0.19 MN
MAE	0.08 MN
MAPE	0.05%

Speedup	$10^6\times$

Monte Carlo sampling with $N = 10^7$ iterations via the surrogate yield's actionable vulnerability probabilities: P (Slight Damage) = 98.5 %, P (Moderate Damage) = 80.2 %, P (Serious Damage) = 0.0008 % (J. Zhang, Jing, et al., 2025). A single LS-DYNA impact analysis requires four to eight hours on modern workstations while the XGBoost surrogate executes in milliseconds, enabling practical vulnerability assessment with 10^7 iterations that would be prohibitively expensive through direct finite element analysis (J. Zhang, Jing, et al., 2025),(LIU Zongfeng et al., 2020). Figure 1 demonstrates the exceptional accuracy of this approach through three complementary visualizations of model performance, including the predicted versus actual scatter plot with $R^2 = 0.996$, residuals analysis confirming unbiased predictions, and feature importance rankings showing the relative influence of input parameters.

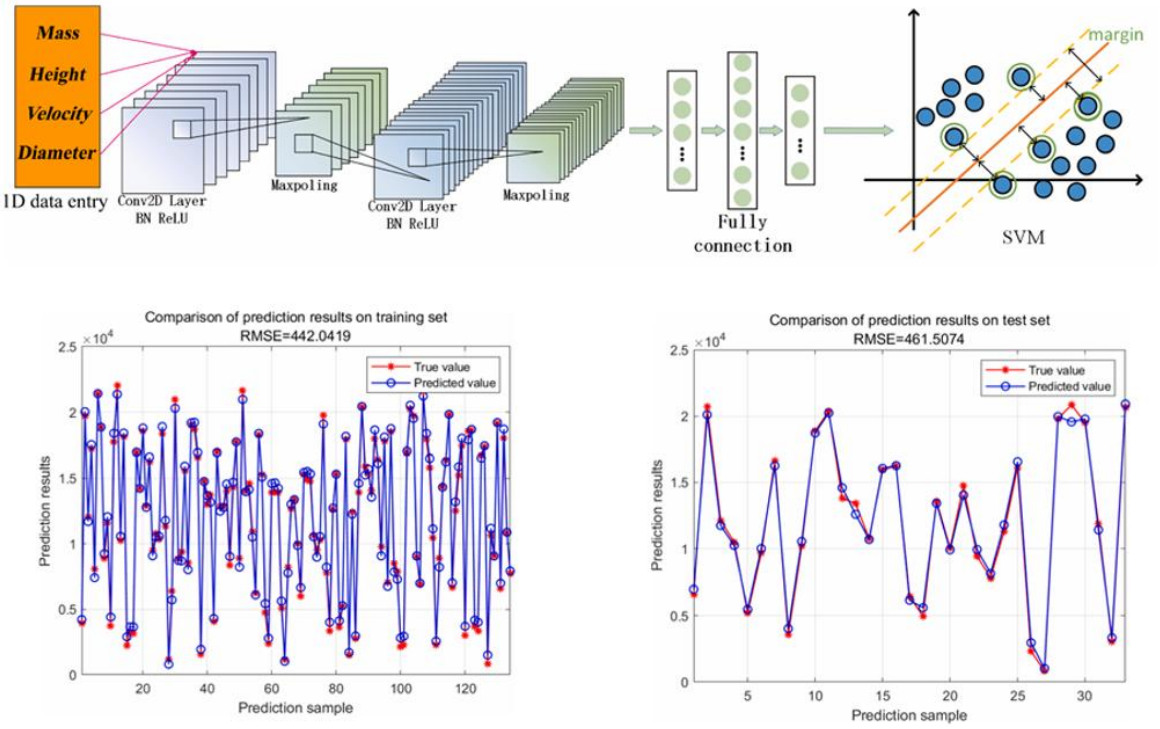

Figure 1: (a) Training-set Prediction Comparisons and (b) Test set prediction results comparison (J. Zhang, Mo, et al., 2025)

Figure 1 Machine Learning Surrogate Accuracy Predictions vs Actual Residual Capacity. Scatter plot of 167 test samples demonstrates exceptional model performance with $R^2 = 0.996$, indicating nearly perfect prediction capability. Linear regression fit confirms unbiased predictions across the entire residual capacity range from 0 to 9100 kilonewtons, validating the XGBoost surrogate for practical vulnerability assessment.

Parametric Sensitivity & Optimal Engineering Demand Parameters

Parametric analysis of 72 scenarios reveals a clear sensitivity hierarchy across design variables. Stirrup spacing demonstrates the most influential effect with 43 percent rupture-width variation across the practical range of 100 to 200 millimeters (J. Zhang, Mo, et al., 2025),(Olsen et al., 2020). This reflects the mechanics of shear-transfer in reinforced concrete panels where closely spaced stirrups distribute impact load over more rebar crosses and reduce stress concentration. Rockfall mass measured through diameter produces approximately two times displacement variation when eight times mass increase is examined (Zhao et al., 2024). Impact velocity produces approximately 1.5 times displacement variation when four times velocity increase is examined. Impact elevation produces less than 10 percent force variation (Mo et al., 2025),(Dhote et al., 2025). Longitudinal reinforcement produces approximately zero percent effect on localized damage when the rockfall diameter is less than the front-panel width, reflecting slab-action-dominated response (Zhao et al., 2024). The axial force ratio and confinement effects remain secondary to these primary variables (G. Zhang et al., 2025),(J. Zhang, Mo, et al., 2025).

The optimal engineering demand parameter (EDP) is residual normalized deflection at the impact location. This parameter exhibits the highest correlation with RVLCC with $r = 0.92$, representing nearly perfect linear relationship, compared to eight other candidate engineering demand parameters evaluated (J. Zhang, Jing, et al., 2025). The optimal EDP is mathematically defined in Equation (3)(J. Zhang, Mo, et al., 2025):

$$\delta_{res}^{il} = \frac{d_{res}^{il}}{H} \quad (3)$$

Where d_{res}^{il} is the permanent displacement at the impact point following rockfall impact and H is the pier height. Eq (3) provides a simple ratio expressing permanent deformation relative to pier height, making it practical for field implementation. It remains measurable via displacement potentiometers or linear variable differential transformer sensors in field damage assessments, enabling practical application without requiring extensive structural analysis (J. Zhang, Mo, et al., 2025).

The relationship between δ_{res}^{il} and normalized residual capacity follows a bilinear pattern that captures two distinct damage regimes. This model, presented in Eq (4) (J. Zhang, Mo, et al., 2025), exhibits $R^2 = 0.91$ across all 72 numerical scenarios:

$$loss = \begin{cases} 0.85\delta_{res}^{il} & if\ \delta_{res}^{il} < 0.012 \\ 1.0 - 1.15e^{-8.5\delta_{res}^{il}} & if\ \delta_{res}^{il} \geq 0.012 \end{cases} R^2 = 0.91 \quad (4)$$

Eq (4) captures the transition from repairable to severe damage at the critical inflection point. The inflection points at $\delta_{res}^{il} = 0.012$ (1.2% of pier height) corresponds to the transition from moderate damage that is repairable to severe damage that requires major structural intervention. In the linear region where $\delta_{res}^{il} < 0.012$, damage accumulates approximately linearly with residual deflection and capacity loss is recoverable through targeted repairs. In the exponential region where $\delta_{res}^{il} \geq 0.012$, damage exhibits accelerating nonlinearity and capacity loss approaches complete failure asymptotically. These relationships are illustrated in **Error! Reference source not found.**, which displays the scatter plot of

72 scenarios, bilinear regression fit with the critical inflection point, and performance objectives mapped to deflection ranges.

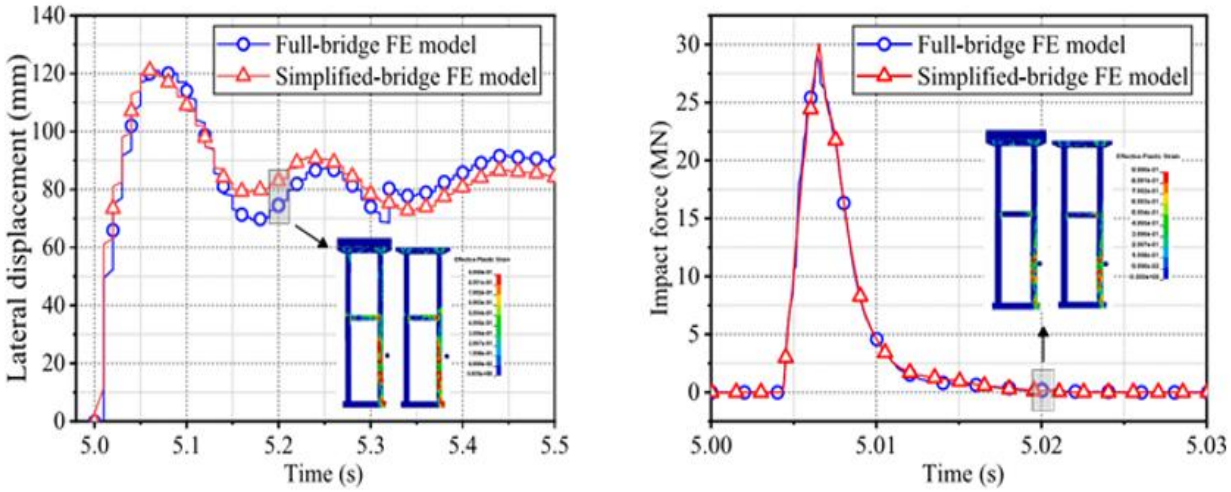

Figure 2: (a) Displacement time history diagram and (b) Impact force time history diagram (J. Zhang, Jing, et al., 2025)

Figure 2: Parametric Sensitivity and Critical Damage Threshold. Scatter plot of 72 earthquake-rockfall cascade scenarios reveals natural clustering around critical inflection point at$\delta_{res}^{il} = 0.012$(1.2% of pier height). This threshold marks the transition from linear damage accumulation (repairable damage regime, $\delta_{res}^{il} < 0.012$) to exponential damage progression (severe damage regime, $\delta_{res}^{il} \geq 0.012$). The critical threshold provides practical design guidance for distinguishing repair-worthy damage from severe damage requiring major structural intervention.

Performance-Based Design Framework

Performance-based design philosophy has successfully transformed earthquake engineering practice by defining multiple structural performance objectives mapped to earthquake intensities (X. Zhang et al., 2021). This paradigm can be adapted to rockfall-impact design through three impact-resistance performance objectives (J. Zhang, Mo, et al., 2025),(Li et al., 2022). The first objective is immediate occupancy where the reinforced concrete bridge pier sustains no damage or only slight damage retaining its original strength and stiffness with RVLCC > 0.95, applies to critical routes such as emergency arteries and lifelines. The second objective is repairable damage where the pier sustains moderate damage while maintaining adequate residual capacity for superstructure support with $0.70 < RVLCC \leq 0.95$, applies to primary routes with regional significance. The third objective is collapsing prevention where the pier sustains severe damage while retaining sufficient residual axial load-bearing capacity to prevent structural collapse with $0.40 < RVLCC \leq 0.70$, applies to secondary or rural routes.

The design procedure comprises six sequential steps. Step one involves hazard characterization through integrated field surveys, remote sensing using light detection and ranging technology and aerial photography, and rockfall trajectory simulation to define the distribution of impact parameters (Z. Liu et al., 2024). Step two requires selection of target performance objective based on bridge criticality classification and project budget constraints. Step three involves pier design parameter determination where diameter$D$, concrete

strength f_c , reinforcement configuration with longitudinal steel ratio and stirrup spacing are proposed while ensuring seismic design requirements are satisfied (X. Zhang et al., 2021). Step four requires estimation of peak rockfall impact force through employment of the CNN-SVM neural network model or unified geometric-structural framework to predict impact force for site-specific rockfall parameters (J. Zhang, Jing, et al., 2025),(LIU Zongfeng et al., 2020). The damage index is calculated using Eq (5):

$$\gamma_D = \frac{v_{dsd}}{v_{dsc}^M} = \frac{F_{impact} A_{contact}}{N_{dyn} b} \quad (5)$$

Where v_{dsd} is the shear demand from impact loading, v_{dsc}^M is the dynamic shear capacity modified for strain rate effects, F_{impact} is the peak impact force, $A_{contact}$ is the contact area, N_{dyn} is the dynamic axial force, and b is the section width. Eq (5) represents the fundamental demand-to-capacity ratio that guides design acceptance or rejection. Step five involves damage index calculation where γ_D quantifies the demand-to-capacity margin. Step six involves performance verification where calculated damage index is compared against performance objective and the design is either accepted or redesigned through iterative adjustment (J. Zhang, Mo, et al., 2025).

The performance-based design framework was demonstrated on a typical mountain expressway bridge with twin rectangular reinforced concrete piers with initial diameter 1200 mm and height 12 meters. With initial design parameters of diameter 1200 mm, concrete strength 35 megapascals, and stirrups number 20 at 150 mm spacing, the dynamic shear capacity is 6655 KN. As presented in Table 3, the iterative design process demonstrates systematic progression toward acceptable performance (J. Zhang, Mo, et al., 2025):

Table 3 Design Iteration Process

Design phase	D (mm)	f_c	s_v	γD	Status
Initial	1200	35	150	1.70	unacceptable
Iteration 1	1400	35	150	1.44	unacceptable
Iteration 2	1200	40	100	1.40	marginal
Final	1300	40	100	1.24	P2 acceptable

The initial design with damage index 1.70 predicts severe unacceptable damage. When the diameter is increased to 1400 mm while maintaining other parameters, the damage index becomes 1.44, which remains unacceptable. Reverting to diameter 1200 mm with concrete strength increased to 40 megapascals and stirrup spacing decreased to 100 mm achieves damage index 1.40, which remains marginally unacceptable. The final design combining improvements with diameter 1300 mm,

concrete strength 40 megapascals, stirrup spacing 100 mm, and increased longitudinal reinforcement achieves damage index 1.24, which is acceptable for the P2 objective predicting moderate damage. The cost increase over the initial design is approximately 12 %. This case exemplifies how the performance-based framework guides economically viable design without resorting to brute-force over-design (J. Zhang, Mo, et al., 2025).

Vulnerability Assessment & Risk Quantification

Monte Carlo sampling with $N = 10^7$ scenarios drawn from the joint geological-structural distribution via XGBoost surrogate yields bridge vulnerability across damage levels (J. Zhang, Jing, et al., 2025),(LIU Zongfeng et al., 2020). The analysis generates 10 million impact scenarios reflecting realistic combinations of rockfall mass, velocity, height, and angle at the bridge location. The damage index calculated for each scenario is converted to probability of exceeding each damage threshold, providing fragility curves and vulnerability information essential for infrastructure risk management (J. Zhang et al., 2022). As documented in Table 4 the probability distribution and reliability indices are summarized showing vulnerability for each damage level. The results reveal that under the site-specific rockfall hazard profile, the bridge has an 80.2 percent probability of exceeding moderate damage. The reliability index of negative 0.85 for moderate damage indicates unacceptable risk by traditional seismic engineering standards and signals urgent need for protective measures. Importantly, complete failure probability remains negligible at 0.0044 percent, indicating that despite substantial damage potential, catastrophic collapse is unlikely, thereby bridging repair and loss-of-life consequences (J. Zhang, Mo, et al., 2025).

Table 4 Bridge Vulnerability Assessment

Damage Level	Probability	Reliability Index β
Basically Intact	1.000	−5.22
Slight Damage	0.985	−2.18
Moderate Damage	0.802	−0.85
Serious Damage	0.0008	3.15

Table 4 provides comprehensive visualization of the vulnerability assessment including fragility curves, probability distributions, and reliability indices mapping to performance objectives.

Figure 3: Bridge Vulnerability Assessment and Probability Distribution. Panel (a) displays fragility curves depicting probability of exceeding four damage thresholds (Basically Intact, Slight Damage, Moderate Damage, Serious Damage) as a function of engineering demand parameter. Panel (b) shows probability distribution from site-specific rockfall hazard analysis: P (Basically Intact) = 1.000, P (Slight Damage) = 0.985, P (Moderate Damage) = 0.802, and P (Serious Damage) = 0.0008, indicating high likelihood of moderate damage requiring repair before traffic restoration under expected loading conditions.

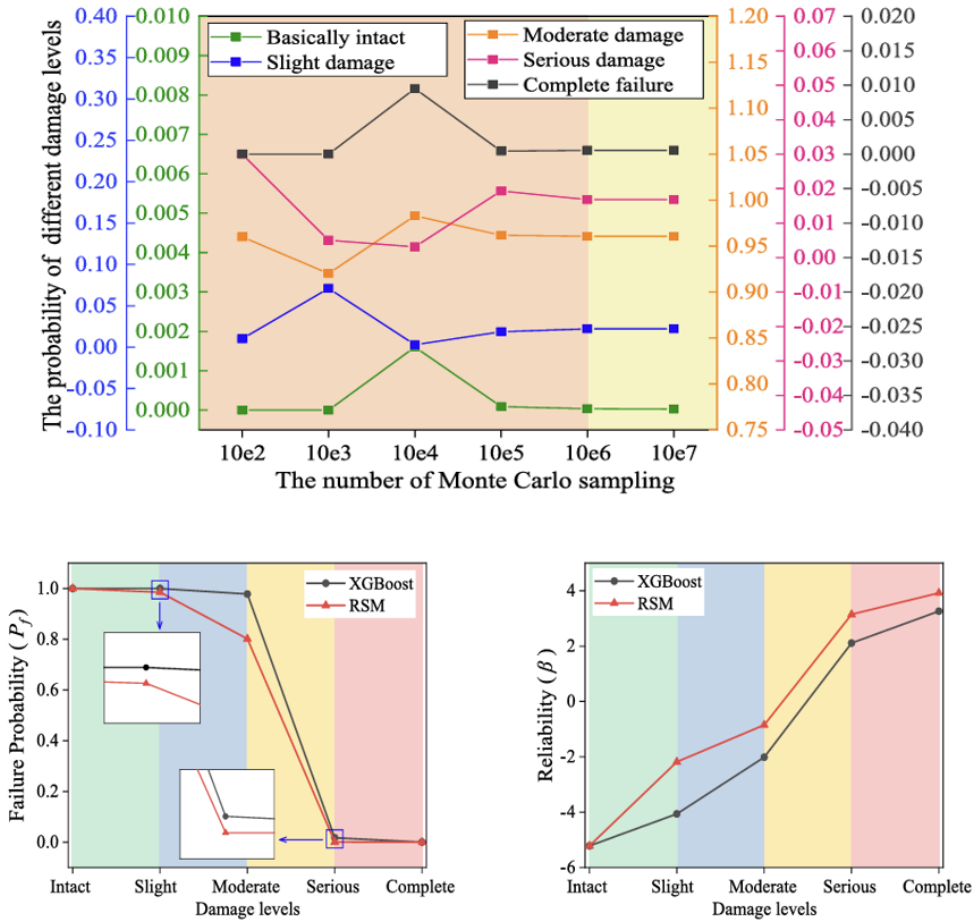

Figure 3: Analysis results under different surrogate models (a) Failure probability P_f ,(b) Reliability β (J. Zhang, Jing, et al., 2025)

Research Gaps and Future Directions

Machine learning generalization represents a critical limitation of current surrogates where models trained on one geometry such as 1200 mm circular hollow piers often fail for different geometries including rectangular sections or T-shaped configurations (J. Zhang, Jing, et al., 2025),(LIU Zongfeng et al., 2020),(Yang et al., 2023). Physics-informed neural networks embedding conservation laws show promise but remain underexplored in structural engineering contexts (J. Zhang, Mo, et al., 2025),(L. Liu et al., 2024). Real rock properties including fracture, deformability, and surface irregularity significantly affect impact response compared to the simplified rigid-sphere assumption in current models, requiring large-scale tests with actual rocks to calibrate the contact algorithms (Zhao et al., 2023),(Gangolu et al., 2022).

Damage index standardization remains a significant gap where existing indices inadequately capture strain-rate and inertial effects dominating impact response (G. Zhang et al., 2025). A unified damage index must incorporate strain-rate hardening factors as function of strain rate history, cumulative plastic strain reflecting micro-void nucleation and coalescence, stress triaxiality capturing confinement-dependent fracture mechanics, and impact duration and rebound interactions for multiple-contact events (J. Zhang, Jing, et al., 2025). Experimental validation

through large-scale impact tests would be essential for calibration(Mo et al., 2025).

Integrated geological-structural assessment remains largely decoupled where slope stability affects rockfall frequency, stochastic rockfall frequency follows non-Poisson arrival processes, damage-dependent bridge capacity degradation requires temporal evolution analysis, and network-level resilience remains unexplored (J. Zhang et al., 2022),(Zhao et al., 2024). These coupled effects require development of integrated frameworks linking geohazard models with structural vulnerability assessment and transportation network consequences (X. Zhang et al., 2021).

Experimental validation through centrifuge testing using 50-gram systems for one-fiftieth-scale models can maintain stress-level similitude while testing pier-slope systems. Full-scale field testing in active rockfall zones with protective barriers for personnel safety should monitor natural impacts via accelerometers and high-speed cameras (Wu et al., 2025),(Mo et al., 2025). Dynamic material property characterization should develop databases of impact properties for common materials in mountainous regions including concrete tensile strength at $1000s^{-1}$, rebar strain-rate hardening for thermomechanical controlled processing steel grades, and rock fracture toughness.

International standards bodies including ISO and the Comité Européen de Normalisation (CEN) should convene working groups developing consensus fragility models parameterized by impact parameters, performance-based design frameworks adapted from seismic engineering, and surrogate modelling guidelines (J. Zhang et al., 2022). Integration into design codes including the International Building Code and Eurocode would accelerate adoption and harmonize global practice (J. Zhang et al., 2022).

Conclusion

Recent advances have transformed rockfall-impact assessment from subjective engineering judgment to quantitative probabilistic frameworks enabling evidence-based decision-making. Key contributions include clear establishment of failure mechanism duality distinguishing localized front panel damage from global response. Identification of the optimal engineering demand parameter as residual normalized deflection at the impact location achieves $r = 0.92$ correlation with RVLCC. Development of XGBoost surrogates with $R^2 = 0.996$ enables rapid vulnerability assessment through Monte Carlo sampling at computational cost one million times lower than direct finite element analysis. Demonstration of performance-based design shows economically viable solutions with realistic cost-benefit. Quantification of earthquake-rockfall cascade effects reveals 83 % non-additive reduction in residual capacity, highlighting critical gaps in current design standards.

Despite rapid recent progress, several fundamental questions persist. Machine learning generalization across heterogeneous pier geometries remains uncertain. Real rock properties including fracture and deformability require systematic investigation. Standardized damage-performance indices accounting for dynamic strain-rate effects remains absent. Integration of geological and structural disciplines through coupled modelling frameworks is needed. International collaboration through standards bodies is essential for code integration and harmonized global practice.

The field is positioned for advancement in physics-informed neural networks embedding conservation laws, digital twin technology integrating wireless sensors with real-time simulation for early warning systems, artificial intelligence interpretability through attention mechanisms and saliency analysis for practitioner confidence, and standardization and code integration through international working groups. These advances would transform rockfall-impact assessment from specialized research to routine engineering practice supported by regulatory standards and design codes applicable globally.

References

Chen, L., Wu, H., & Liu, T. (2020). Shear Performance Evaluation of Reinforced Concrete Piers Subjected to Vehicle Collision. *Journal of Structural Engineering*, *146*(4), 04020026.

https://doi.org/10.1061/(ASCE)ST.1943-541X.0002571

Dhote, K. D., Verma, P. N., & Suryawanshi, M. V. (2025). *14th International Symposium on Plasticity and Impact Mechanics*.

Fan, W., Liu, B., & Consolazio, G. R. (2019). Residual Capacity of Axially Loaded Circular RC Columns after Lateral Low-Velocity Impact. *Journal of Structural Engineering*, *145*(6), 04019039. https://doi.org/10.1061/(ASCE)ST.1943-541X.0002324

Gangolu, J., Kumar, A., Bhuyan, K., & Sharma, H. (2022). Probabilistic demand models and performance-based fragility estimates for concrete protective structures subjected to missile impact. *Reliability Engineering & System Safety*, *223*, 108497. https://doi.org/10.1016/J.RESS.2022.108497

Jibson, R. W., Harp, E. L., & Michael, J. A. (n.d.). *A Method for Producing Digital Probabilistic Seismic Landslide Hazard Maps: An Example from the Los Angeles, California, Area Open-File Report 98-113*.

Li, F., Liu, Y., & Yang, J. (2022). *Durability Assessment Method of Hollow Thin-Walled Bridge Piers under Rockfall Impact Based on Damage Response Surface*. https://doi.org/10.20944/preprints202209.0274.v1

Liu, L., Zhao, X., Hu, T., Liang, F., Guo, B., & Tao, K. (2024). Deep-learning-assisted self-powered wireless environmental monitoring system based on triboelectric nanogenerators with multiple sensing capabilities. *Nano Energy*, *132*. https://doi.org/10.1016/j.nanoen.2024.110301

Liu, Z., Wang, M., Chen, K., Demartino, C., Li, Y., & Nikitas, N. (2024). Dynamic Analysis of Rockfall Impact on Bridges: Implications for Train Safety. *International Journal of Structural Stability and Dynamics*. https://doi.org/10.1142/S0219455425410056

Liu, Z., Wang, M., Wang, L., Demartino, C., Chen, H., Hu, R., Hasan, N., Nikitas, N., Bourrier, F., & Li, Y. (2025). *Dynamic Performance and Optimization of a Novel Flexible Shed Tunnel for Enhanced Rockfall Protection of Bridges*.

Liu Zhanhui, Hu Ruijie, Yao Changrong, Li Yongle, & Li Yadong. (2020). *State of the art review of bridge impact research in 2019*.

LIU Zongfeng, CHEN Yingtao, & YANG Shaojun. (2020). *Study on Pulse Impact Protection Scheme for " Two-tunnel and one-bridge" High-speed Railway Falling Rock*.

Ma, R., Dong, H., Wen, J., Du, X., Han, Q., & Wen, 8 3 Jianian. (n.d.). *Investigations on the Residual Vertical Load-Carrying Capacity for RC 2 Two-column Bridge Bents under Earthquake-Rockfall Cascading Hazards*. https://ssrn.com/abstract=5248553

Mo, Y., Han, Y., Zhang, J., Zhang, Z., & Wu, W. (2025). Dynamic response analysis of hollow thin-walled pier rigid-frame bridge under rockfall impacts. *Advances in Bridge Engineering*, *6*(1). https://doi.org/10.1186/s43251-025-00178-0

Olsen, M. J., Massey, C., Senogles, A., Leshchinsky, B. A., & Wartman, J. (2020). *PREDICTING SEISMIC-INDUCED ROCKFALL HAZARD FOR TARGETED SITE MITIGATION Final Report Draft SPR-809*.

Technical Background Report. (2002).

Wu, J., Ye, F., Yang, J., Xu, J., Wu, J., Ye, F., Yang, J., & Xu, J. (2025). Dynamic Response and Residual Bearing Capacity of Corroded RC Piers Under Rockfall Impact. *Buildings 2025, Vol. 15, 15*(15). https://doi.org/10.3390/BUILDINGS15152592

Yang, G., Yang, R., & Zhang, J. (2023). Prediction and Interpretation of Residual Bearing Capacity of Cfst Columns under Impact Loads Based Interpretable Stacking Fusion Modeling. *Buildings*, *13*(11). https://doi.org/10.3390/buildings13112783

Zhang, G., Zhang, J., & He, C. (2025). Damage and protection of simply supported girder bridge pier: Rockfall impact. *Structures*, *82*. https://doi.org/10.1016/j.istruc.2025.110461

Zhang, J., Jing, Y., Ma, J., Luo, J., Bao, H., & Chen, S. (2025). Machine learning enhanced bridge vulnerability quantification under rockfall hazards. *Engineering Geology*, *352*. https://doi.org/10.1016/j.enggeo.2025.108066

Zhang, J., Mo, Y., Huang, H., & Wu, W. (2025). Performance-based damage indices and optimization design framework for Rockfall-Resistant RC Twin-Column bridge piers. *Engineering Failure Analysis*, *182*. https://doi.org/10.1016/j.engfailanal.2025.110026

Zhang, J., Wang, R., Han, W., & Bao, H. (2022). A comprehensive approach for bridge performance evaluation under rockfall impact integrated with geological hazard analysis. *Engineering Failure Analysis*, *141*. https://doi.org/10.1016/j.engfailanal.2022.106668

Zhang, X., Wang, X., Chen, W., Wen, Z., & Li, X. (2021). Numerical study of rockfall impact on bridge piers and its effect on the safe operation of high-speed trains. *Structure and Infrastructure Engineering*, *17*(1), 1–19. https://doi.org/10.1080/15732479.2020.1730406

Zhao, W., Feng, H., Ye, J., & Qian, J. (2023). Dynamic responses and damage behavior of hollow RC piers against rockfall impact. *Thin-Walled Structures*, *187*. https://doi.org/10.1016/j.tws.2023.110771

Zhao, W., Li, W., Feng, H., Ye, J., Lan, G., & Qian, J. (2024). Residual performance of hollow RC piers damaged by rockfall impact. *Structures*, *59*. https://doi.org/10.1016/j.istruc.2023.105726

Zhong, H., Hao, C., Yu, Z., Lyu, L., & Wu, A. (2023). Damage assessment of RC bridge piers under rockfall impact and evaluation of a steel-sand protective structure. *Structures*, *47*, 607–624. https://doi.org/10.1016/j.istruc.2022.11.100